AD-A082 888 JOHNS HOPKINS UNIV LAUREL MD APPLIED PHYSICS LAB F/G 22/3
DRAG ESTIMATION AND SATELLITE ORBIT DETERMINATION.(U)
MAR 80 A EISNER N00024-78-C-5384
UNCLASSIFIED JHU/APL/TG-1327 NL

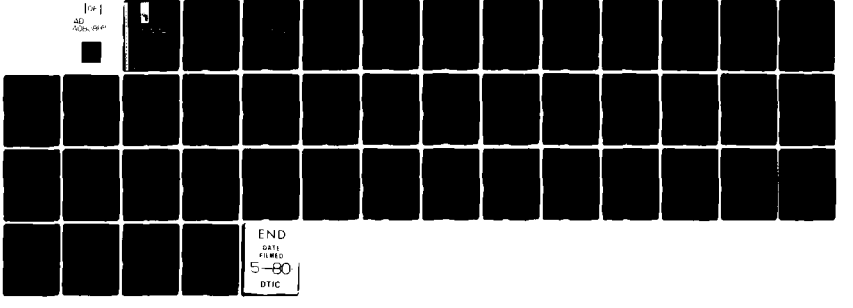

END
DATE FILMED
5-80
DTIC

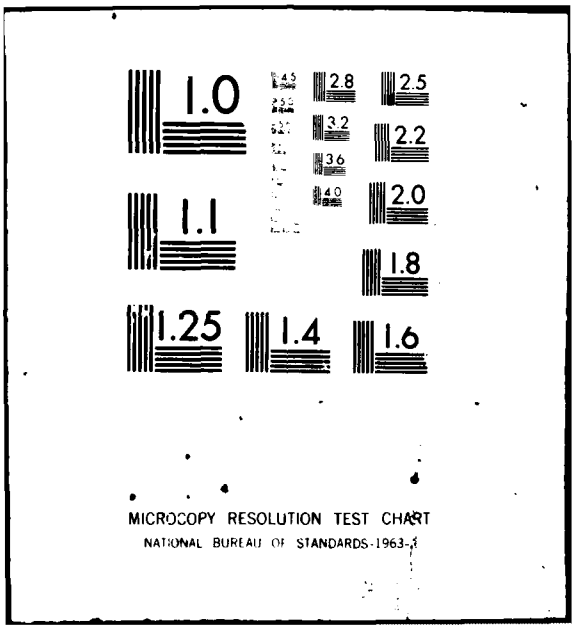
1.0
2.8
2.5
3.2
2.2
3.6
4.0
2.0
1.1
1.8
1.25
1.4
1.6
MICROCOPY RESOLUTION TEST CHART
NATIONAL BUREAU OF STANDARDS-1963-A

JHU/APL
TG 1327
MARCH 1980
Copy No. 1

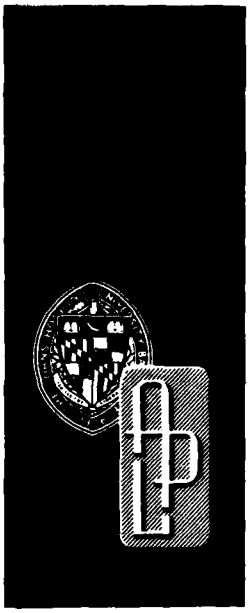

Technical Memorandum

DRAG ESTIMATION AND SATELLITE ORBIT DETERMINATION

A. EISNER

THE JOHNS HOPKINS UNIVERSITY ■ APPLIED PHYSICS LABORATORY

Unclassified

SECURITY CLASSIFICATION OF THIS PAGE

PLEASE FOLD BACK IF NOT NEEDED FOR BIBLIOGRAPHIC PURPOSES

REPORT DOCUMENTATION PAGE

1. REPORT NUMBER: JHU/APL/TG-1327	2. GOVT ACCESSION NO	3. RECIPIENT'S CATALOG NUMBER
4. TITLE (*and Subtitle*): DRAG ESTIMATION AND SATELLITE ORBIT DETERMINATION		5. TYPE OF REPORT & PERIOD COVERED: Technical Memorandum
		6. PERFORMING ORG. REPORT NUMBER
7. AUTHOR(s): A. Eisner		8. CONTRACT OR GRANT NUMBER(s): N00024-78-C-5384
9. PERFORMING ORGANIZATION NAME & ADDRESS: The Johns Hopkins University Applied Physics Laboratory, Johns Hopkins Rd., Laurel, Md. 20810		10. PROGRAM ELEMENT, PROJECT, TASK AREA & WORK UNIT NUMBERS: Task S1X0
11. CONTROLLING OFFICE NAME & ADDRESS: Strategic Systems Project Office, SP-243, Washington, D.C. 20376		12. REPORT DATE: March 1980
		13. NUMBER OF PAGES: 47
14. MONITORING AGENCY NAME & ADDRESS: Naval Plant Representative Office, Johns Hopkins Rd., Laurel, Md. 20810		15. SECURITY CLASS. (*of this report*): Unclassified
		15a. DECLASSIFICATION/DOWNGRADING SCHEDULE
16. DISTRIBUTION STATEMENT (*of this Report*): Approved for public release; distribution unlimited.		
17. DISTRIBUTION STATEMENT (*of the abstract entered in Block 20, if different from Report*)		
18. SUPPLEMENTARY NOTES		

19. KEY WORDS (*Continue on reverse side if necessary and identify by block number*)

Transit	Density	Ephemeris
Drag	Tracking	
Satellite	Orbit determination	
Atmosphere	Navigation	

20. ABSTRACT (*Continue on reverse side if necessary and identify by block number*)

Like the weather, upper atmospheric density often behaves unpredictably. Even the best models of the upper atmosphere cannot consistently predict atmospheric density for Transit System satellites (1000 km) to the desired high precision.

A comprehensive evaluation is presented of the drag estimation concept as a tool in routinely determining the orbit of the Transit System; the benefits to the Transit System are also examined. The resulting data (fitted along-track bias force) can be used subsequently to study upper atmospheric density variations at Transit satellite altitudes that will lead ultimately to improved upper atmospheric density models.

Drag estimation in satellite orbit determination yields higher precision-tracked (determined) ephemerides and significantly improves the prediction (extrapolated satellite position) accuracy of the Transit System.

DD FORM 1 JAN 73 1473

Unclassified

SECURITY CLASSIFICATION OF THIS PAGE

JHU/APL
TG 1327
MARCH 1980

Technical Memorandum

DRAG ESTIMATION AND SATELLITE ORBIT DETERMINATION

A. EISNER

THE JOHNS HOPKINS UNIVERSITY ■ APPLIED PHYSICS LABORATORY
Johns Hopkins Road, Laurel, Maryland 20810
Operating under Contract N00024-78-C-5384 with the Department of the Navy

ABSTRACT

Like the weather, upper atmospheric density often behaves unpredictably. Even the best models of the upper atmosphere cannot consistently predict atmospheric density for Transit System satellites (1000 km) to the desired high precision.

A comprehensive evaluation is presented of the drag estimation concept as a tool in routinely determining the orbit of the Transit System; the benefits to the Transit System are also examined. The resulting data (fitted along-track bias force) can be used subsequently to study upper atmospheric density variations at Transit satellite altitudes that will lead ultimately to improved upper atmospheric density models.

Drag estimation in satellite orbit determination yields higher precision-tracked (determined) ephemerides and significantly improves the prediction (extrapolated satellite position) accuracy of the Transit System.

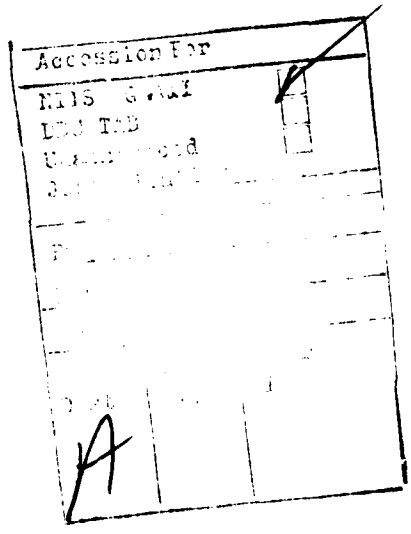

CONTENTS

ILLUSTRATIONS

TABLES

1. INTRODUCTION

It has become apparent that a complete and accurate representation of the effects of drag on satellites is lacking. Even the best models of the atmosphere cannot duplicate the actual prevailing conditions at satellite altitudes. An alternative (or addition) to modeling the atmosphere is to eliminate its effects on satellites by using "drag estimation," which is the inclusion of a drag parameter in the satellite orbit determination process. The resulting fitted parameter is used to generate an along-track force correction, thereby compensating for the shortcomings of the drag model.

Errors in the modeled drag force result in along-track satellite position errors that grow quadratically with time (see Appendix A). Figure 1 illustrates some typical fixed-site, along-track navigation results that are proportional (and nearly identical) to the satellite along-track position errors. The orbit determination interval gives a measure of the satellite position errors after an orbit adjustment. The ephemeris extrapolation interval shows a quadratic growth in time (centered at the middle of the track) and gives a measure of satellite position errors before an orbit adjustment.

Without drag estimation, the theoretical function used in the orbit determination process includes constant and linear (in time) terms. The resulting fitted parameters are converted to corrections to the satellite semimajor axis (linear term) and mean anomaly (constant term). Nothing has been done about the quadratic growth that is evident in the track and that results in serious errors at the end of the prediction span. Drag estimation includes in the fitting process an additional term that grows quadratically in time. The resulting fitted parameter can then be converted into an along-track force correction (correction to the modeled drag force), which is handled like any other force acting on the satellite.

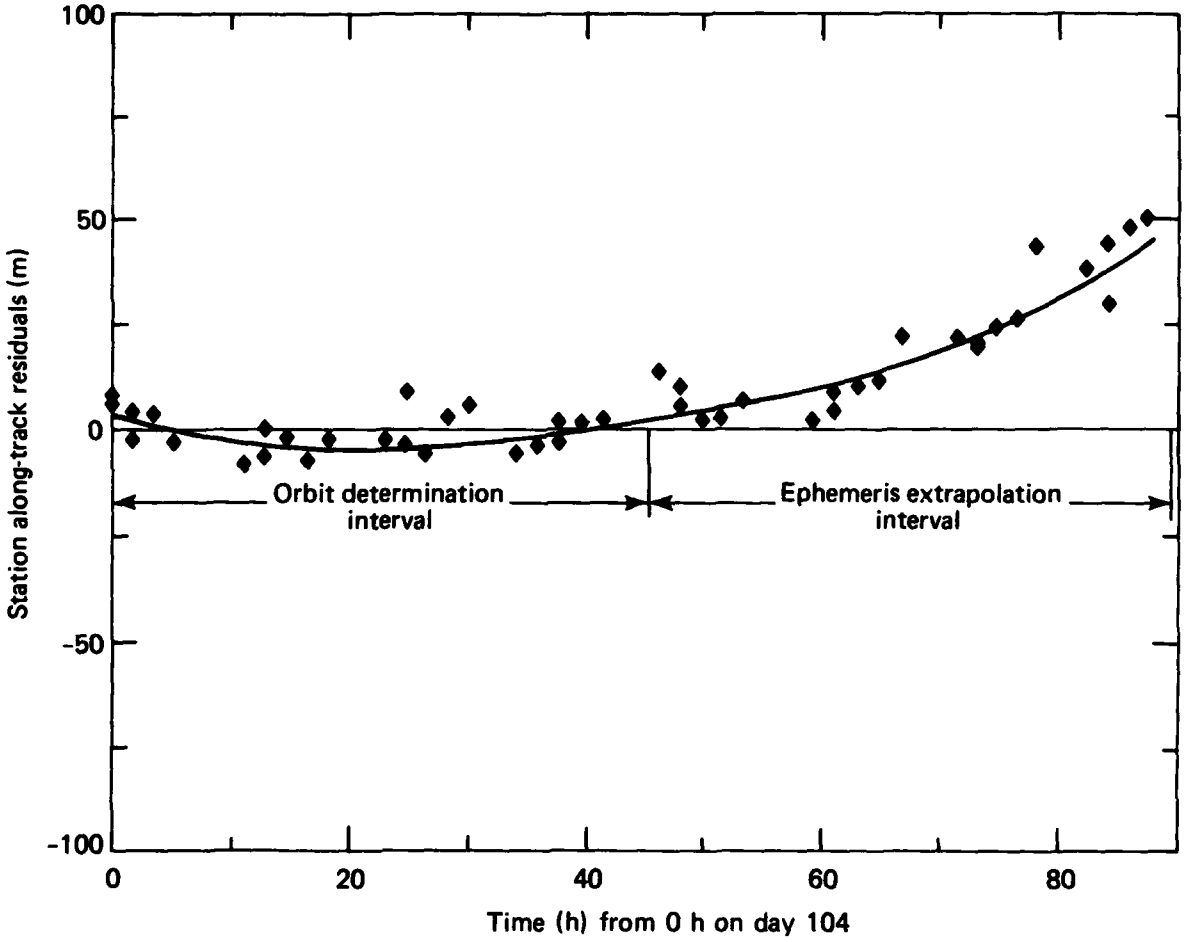

Fig. 1 Along-track navigation residuals for satellite 30120 in 1978.

2. SUMMARY AND CONCLUSION

Drag estimation is a viable concept that can be implemented and used routinely in the orbit determination process for the Transit System. The primary assumption that forms the basis for the drag estimation technique is that drag model errors vary slowly with time; that is, correlation time is long compared with the orbit determination interval. Results presented here confirm that, on the average, the assumption is valid. Occasionally, however, rapid (compared with the orbit determination interval) changes in the atmosphere result in poor ephemeris extrapolation unless the resulting estimated along-track correction force is intentionally damped to suppress the short-term changes in the atmosphere.

A manual drag estimation system has been used successfully at the Navy Astronautics Group (NAVASTROGRU) since April 1978. The manual procedure involves the routine monitoring of satellite along-track errors (examination of predicted fixed-site along-track navigation errors) and, when necessary, the correction of drag force by changing the coefficient of drag (C_d) from its "true" value of 3.0. Automated (computer-generated) drag estimation removes the guesswork (magnitude of needed changes to C_d), follows short-term (daily) as well as long-term drag model errors, and requires substantially less manual interference. Benefits include higher precision-tracked ephemerides (sometimes referred to as precise ephemerides), improved prediction accuracy (when using the current prediction span), and lengthening the prediction span without loss in (current) system performance. Routine drag tracking produces valuable data (fitted bias forces and mean modeled densities) that are essential for the study of upper atmospheric density variations.

3. BACKGROUND

Drag estimation was first attempted in 1968 in a special version of the Transit System's Orbit Improvement Program (OIP). Its purpose was to supplement the existing drag model and thereby improve orbit prediction accuracy. The drag parameter chosen was C_d, which for the Transit satellites had a nominal value of 3.0. Modeled density errors would be countered by adjusting (fitting) C_d either upward (model underestimating density) or downward (model overestimating density) from its nominal value. The necessary theory (see Appendix A) was developed, and a special drag tracking version of OIP was generated and tested shortly thereafter on NAVASTROGRU's IBM 7094 computer.

The conclusions drawn from that first study are valid today:

1. Drag estimation requires data intervals longer than the currently used 36 h spans.

2. Even with longer spans (44 h), the variation from one span to the next of the fitted values of C_d was too sporadic to be attributed to the uncertainty in the drag model.

3. The linear and quadratic coefficients in the fitted function (a_1 and a_6) cannot be treated independently as was believed previously.

Dramatic improvements in the tracking accuracy of the Transit System were achieved during the intervening years, but repeated attempts to fit a drag parameter have failed to alter the 1968 conclusions. The crux of the problem was the inseparability of the linear and quadratic terms (in time) in the orbit-fitting equation. The concept of fitting out a drag parameter was later replaced with a bias force in HLC coordinates (Appendix A) whose along-track component (L) can be adjusted (on option) along with the other fitting parameters. The same approach was also carried over into the new Orbit Determination Program (ODP), the IBM 360 replacement for OIP, where the ability to fit out an along-track bias force was retained. Recent increases in the sun's activity and the associated variations

in upper atmospheric density have again surfaced to remind us that the upper atmosphere is unpredictable (Ref. 1).

This report reexamines the old approach, introduces a new one and summarizes the results of extensive testing of drag estimation at APL and NAVASTROGRU where the concept is being evaluated for inclusion in the routine operations of the Transit System.

Ref. 1. H. E. Hinteregger, "Development of Solar Cycle 21 Observed in EUV Spectrum and Atmospheric Absorption," J. Geophys. Res., Vol. 84, No. A5, 1 May 1979.

4. THE LATEST ATTEMPTS USING THE OLD APPROACH

In theory, there is no problem in separating the linear from the quadratic growth in the satellite along-track errors. In practice, we have to contend with a number of problems:

1. The data are noisy,

2. The data are sparse (small number of passes) and poorly distributed geographically, and

3. Residual pole position errors introduce a 24 h oscillation into the along-track navigation residuals.

The approach that had been taken previously was to assign quadratically growing, along-track position errors to drag model errors. A bias force in the along-track direction was introduced to compensate for the modeled errors. One difficulty is that the quadratic and linear terms "fight" each other; that is, it is quite common to fit out large compensating quadratic and linear terms. The linear term is converted to an adjustment to the initial semimajor axis (satellite period), and the quadratic term is transformed into an along-track bias force. If we fit out an incorrect (unusually large) quadratic term that is compensated for by an equally large (and opposite in sign) linear term, we will pay the price for these errors in the update (ephemeris extrapolation) interval. The "incorrect" bias force will cause quadratic (in time) growth in the along-track errors that will only be partially compensated for by the equally incorrect though only linearly growing (in time) period error. The result could be disastrous. In a recent test, two out of three consecutive orbit determination runs resulted in poorer predictions when compared to their standard operational counterparts, using four clusters (48 h of data) for orbit determination and ephemeris extrapolation intervals (see Table 1).

In a second test, we added two more clusters (24 h of data) to the orbit determination intervals but kept the extrapolation spans to four clusters (48 h). The results were better; two out of three improved, with the third showing only a slight degradation when compared to the no-drag fitting case (Table 2).

In the runs shown in Tables 1 and 2, we intentionally introduced an error in the drag force by setting the mean solar index to 125, which is 30 units too high. Therefore, we would expect to fit out a bias force in the positive along-track direction (opposite to

Table 1

Drag estimation (includes fit to linear terms) results using 2 days of data.

Satellite	Span (1977) From (day)	(h)	To (day)	(h)	Along-track bias force* ($R_0/s^2 \times 10^{15}$)	rms along-track errors (m), 48 h extrapolation Drag fit	No-drag fit
30140	339	18	341	12	0.29	--	--
	341	18	343	12	0.20	9.7	29.7
	343	16	345	12	0.18	26.2	15.2
	345	16	347	12	0.17	56.0	28.7

*R_0 scaling factor = 6378.166 km

Table 2

Drag estimation (includes fit to linear terms) results using 3 days of data.

Satellite	Span* (1977) From (day)	(h)	To (day)	(h)	Along-track bias force ($R_0/s^2 \times 10^{15}$)	rms along-track errors (m), 48 h extrapolation Drag fit	No-drag fit
30140	338	18	341	12	0.11	--	--
	340	18	343	12	0.17	12.8	29.7
	342	18	345	12	0.12	13.6	15.2
	344	16	347	12	-0.14	35.1	28.7

*Note that the extrapolation span covers only the last 48 h of each orbit determination.

the drag force) to compensate for the error in the drag force (negative along-track direction). It was surprising to find that in the fourth track there was a reversal in the sign of the fitted bias force. A possible explanation will be discussed in the last section of this report.

5. A NEW APPROACH TO THE OLD PROBLEM

The difficulty with getting drag estimation to work is the poor (or incomplete) separation between the linear (period) and quadratic (bias force) parameters in the orbit adjustment process. The linear term (period error) has alway been one of the standard six orbit parameters. The error in the period is corrected by adjusting the semimajor axis. Why is there a period error? Primarily it is because the modeled drag force is less than perfect, and the period (semimajor axis) needs to be corrected along with the other parameters. If the main reasons for adjusting the semimajor axis are errors in the modeled drag force and if errors in the modeled drag force result in quadratic (in time) growth of the along-track position of the satellite, would it not make more sense to fit out a quadratic term and forget the linear term?

To test the validity of the new approach, we repeated the four orbit determination runs and compared the results to the previous set of runs (Tables 1 and 2). The ODP program was designed with the capability to determine all or any subset of 11 parameters. Normally (operationally) we adjust eight parameters (six orbit and two frequency parameters). One of the eight (a_1) is a correction to the semimajor axis (or the linear term). With our new approach, using ODP, we remove a_1 from the fitting space and include instead the along-track bias force parameter (or the quadratic term, a_6). The resulting bias force is then routinely integrated along with the other forces acting on the satellite. Explicit corrections to the semimajor axis (a_1) are neither computed nor applied. The results of the first four orbit determination runs were encouraging; two of the three extrapolated ephemerides showed significant improvement over both of the previous drag estimation attempts (Tables 1 and 2) and the parallel (OIP) no-drag-fit runs. The third was only slightly worse (rms = 18.3 m compared to 15.2 m (see Table 3)).

The results, which warranted the continuation of the experiment for an additional nine intervals (48 h each) or a total of 26 days, were better than we had anticipated. Only one out of the 12 extrapolations was significantly worse (30 m rms compared to 15 m for the OIP run). Eight of the 12 showed significant improvement (5 to 40 m reduction in the predicted rms). The remaining three did about the same (two doing slightly better and one slightly worse). Table 4 summarizes the results. A few observations follow:

Table 3

Drag estimation (excludes fit to linear terms) results using 2 days of data.

Satellite	Span (1977) From (day)	(h)	To (day)	(h)	Along-track bias force ($R_0/s^2 \times 10^{15}$)	rms along-track errors (m), 48 h extrapolation Drag fit	No-drag fit
30140	339	18	341	12	0.11	--	--
	341	18	343	12	0.15	7.5	29.7
	343	16	345	12	0.03	18.3	15.2
	345	16	347	12	-0.11	16.2	28.7

Table 4

Results of drag estimation (excludes fit to linear terms) (ODP) compared with no-drag estimation (OIP).

Satellite	Span (1977) From (day)	(h)	To (day)	(h)	Number of passes Input	Used (ODP/OIP)	Fitted along-track force ($R_0/s^2 \times 10^{15}$) ODP	48 h along-track residuals (m) Orbit determination ephemeris extrapolation rms ODP	OIP	Last pass ODP	OIP	rms ODP	OIP
30140	339	18	341	12	20	20/20	+0.11	3.9	5.3	--	--	--	--
30140	341	18	343	12	25	25/25	+0.16	4.2	3.9	+12.3	+46.1	7.5	29.7
30140	343	16	345	12	27	23/27	+0.03	3.0	4.0	-31.2	+23.1	18.3	15.2
30140	345	16	347	12	26	26/26	+0.11	3.1	3.2	-30.7	-54.6	16.2	28.7
30140	347	16	349	12	25	21/25	+0.12	3.4	5.1	+53.8	-20.5	30.6	15.1
30140	349	16	351	12	24	23/24	+0.09	3.2	4.2	+ 8.0	+26.1	12.2	16.1
30140	351	16	353	12	27	25/24	+0.08	3.0	3.9	+16.8	+28.2	14.4	19.4
30140	353	15	355	9	27	27/28	+0.10	2.9	2.2	+12.3	+38.3	11.1	25.4
30140	355	15	357	11	23	22/23	+0.10	3.0	4.9	+ 6.9	+35.3	5.2	19.6
30140	357	15	359	11	13	13/12	+0.25	3.8	4.1	+35.2	+63.7	20.3	38.5
30140	359	15	361	11	16	16/14	+0.20	3.2	3.8	-15.0	+79.8	8.7	47.8
30140	361	15	363	11	15	14/14	+0.13	4.2	4.5	-16.9	+57.7	11.1	33.7
30140	363	17	365	11	21	19/21	+0.11	3.1	4.7	-22.6	+19.5	14.2	14.8
						Mean	+0.10	3.4	4.1			14.2	25.3
						Standard deviation	0.09	0.5	0.8			6.8	10.7

ODP - drag estimation
OIP - no-drag estimation

1. The average of the orbit determination data residuals improved 0.7 m (17%).

2. The average of the extrapolated data residuals improved 11.1 m (44%).

3. The mean bias force (0.10×10^{-15} R_0/s^2) was about what we expected (compensating for the 30 unit error in the mean solar index).

4. The worst drag-estimation extrapolated ephemeris (30 m, days 347 to 349) was better than three no-drag-estimation extrapolations (33.7, 38.5, and 47.8 m) and about the same as two other no-drag-estimation extrapolations (29.7 and 28.7 m); that is, five of the standard runs did as poorly as or worse than the single worst drag-estimation extrapolated case.

Figure 2 summarizes the results of drag estimation versus no-drag estimation. The superiority of drag estimation is clearly evident. The lower portion of Fig. 2 compares drag estimation to no-drag estimation. The shaded portions outline the areas where drag estimation was superior to no-drag estimation.

It is of interest to speculate on the source of the drag model errors (fitted bias force) by looking for a possible correlation with known variations in the upper atmosphere.

Figure 3 is an attempt to correlate the fitted bias force (correction for drag errors) with the prevailing solar and magnetic indices. First, we can remove one known source of error that we introduced (30 units in the mean solar index), which is equivalent to the 0.10×10^{-15} R_0/s^2 mean fitted bias force. Only four of the 12 intervals deviate significantly from the mean: days 344 to 347 and days 357 to 361. The earlier period coincides with a magnetic storm of moderate intensity, which suggests that the modeled drag force underestimates the effects of magnetic storms (negative bias force). There is no obvious correlation with either the solar or the magnetic index for the latter period (days 357 to 361).

The results of the new approach to drag estimation are exciting and potentially valuable to the Navy Navigation Satellite System (NNSS). We are now in the midst of the most disturbed part of the 11 yr, 21st solar cycle, when the effects of increased mean densities and unpredictable variations in upper atmospheric densities become the rule rather than the exception. Drag models do well under normal circumstances, but they incorporate only known variations and are based on historical (20th solar cycle) rather than current

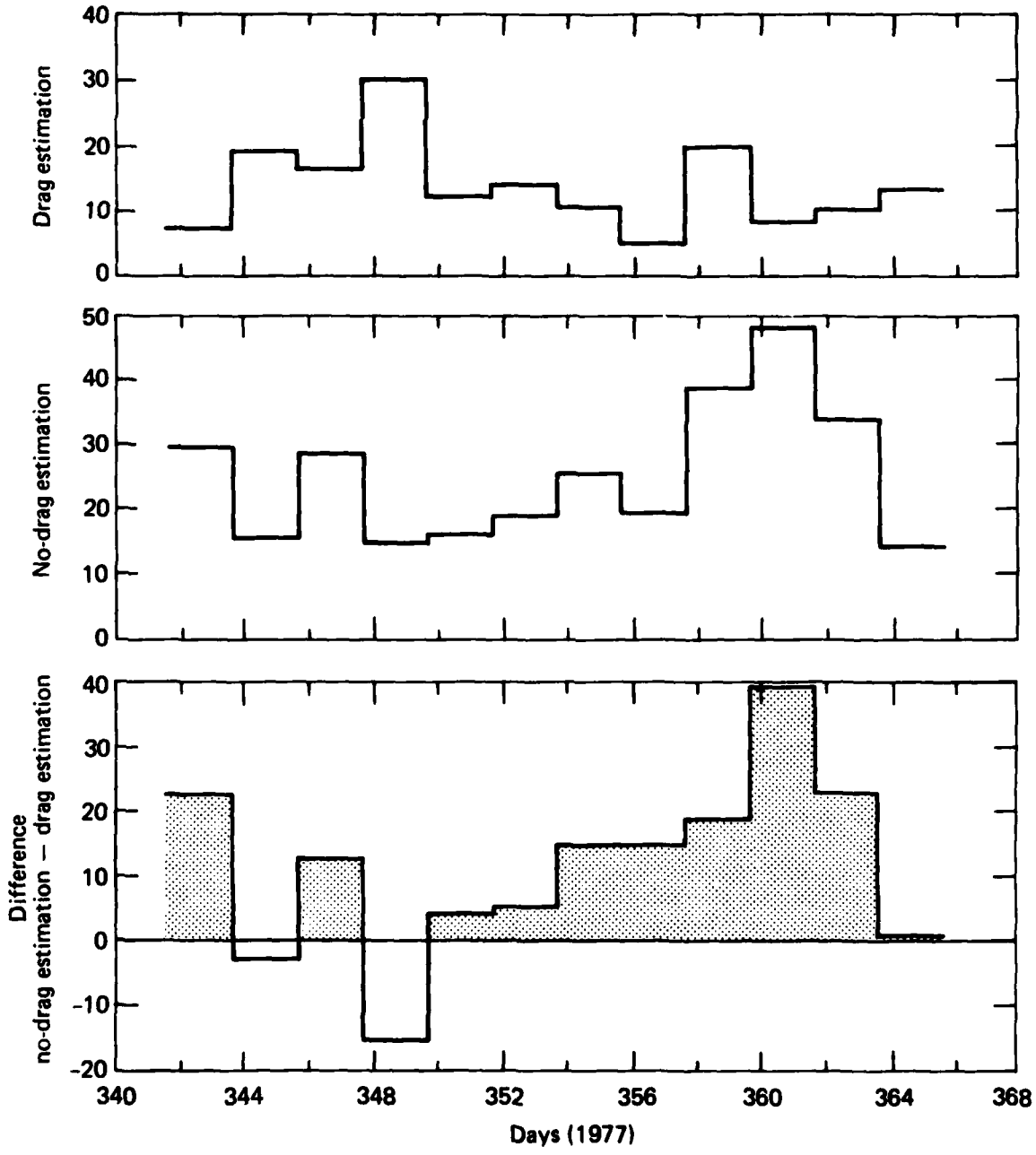

Fig. 2 rms of extrapolated along-track residuals for satellite 30140 (m).

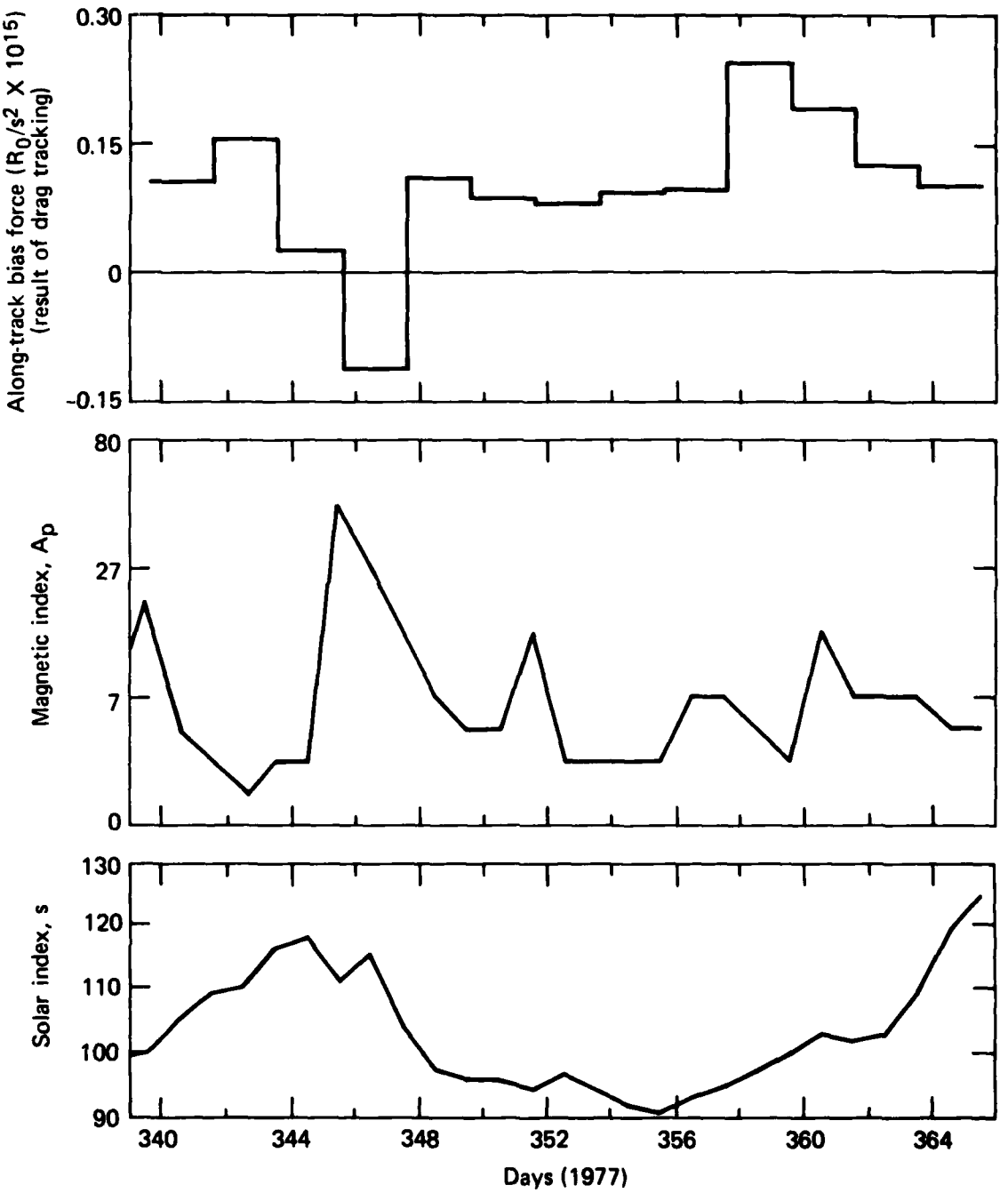

Fig. 3 Fitted along-track bias force and prevailing solar/magnetic conditions for satellite 30140.

data. The next step was to see how well drag tracking would handle a difficult period like that of April 1978 when Transit satellites suffered serious extrapolation errors as a result of drag model errors.

6. THE APRIL 1978 EXPERIMENT

The first 100 days of 1978 were marked by a sudden increase in the sun's activity. The mean solar index almost doubled between November 1977 and April 1978. Daily solar readings reached 190, and several magnetic storms of moderate intensity ($A_p > 50$) were observed. During the same period, the extrapolated ephemerides of the five Transit satellites indicated that the modeled drag force was usually too low. The problem did not surface until early April 1978 when a combination of severe solar and magnetic disturbances resulted in a serious degradation in the accuracy of the predicted (extrapolated) positions of all five satellites. A 20 day span (days 90 to 110, 1978) was chosen, and orbits were determined for all five satellites using the drag estimation option in ODP and the new approach described earlier. Results are summarized in Table 5, and the extrapolated along-track navigation residuals are displayed in Figs. 4 through 8. Orbits were determined for three of the satellites (30120, 30130, and 30140) every other day and for the other two daily. The worst extrapolation errors occurred on days 100 to 103. *Disturbed solar and magnetic conditions* on day 100 are probably responsible for the large extrapolation errors seen on days 100 to 101. No such correlation exists for days 102 to 103, yet the along-track extrapolated positions were the worst for all five satellites (see Table 5). We will postpone the discussion of this point to the last section of the report.

Figure 9 is a plot of the fitted bias force (modeled drag error) for each of the five satellites and the prevailing solar and magnetic conditions for the period. Note the following points of interest:

1. The variations in the fitted bias force (modeled drag force error) are similar for all five satellites (see the dashed line).

2. There is a strong suggestion that the fitted bias force follows the daily variation in the magnetic index, A_p. Peak bias forces were fitted out on days 100 to 101. Day 100 recorded the highest magnetic index ($A_p = 45$). An earlier magnetic peak on day 93 ($A_p = 27$) correlates well with bias force peaks for all but satellite 30140. A late peak on day 103 ($A_p = 31$) also correlates well with (negative) increases in the bias force on day 104. The decline in the magnetic index on the next three days (104 to 106)

Table 5

Orbit determination results for the April 1978 experiment.

Span (1978)		Fitted along-track force ($R_0/a^2 \times 10^{15}$)					rms of along-track prediction errors (m)				
							48 h extrapolation			24 h interval with 24 h extrapolation	
From (day)	To (day)	Sat. 30120	Sat. 30130	Sat. 30140	Sat. 30190	Sat. 30200	Sat. 30120	Sat. 30130	Sat. 30140	Sat. 30190	Sat. 30200
90	91	-0.05	+0.13	+0.11	+0.10	+0.13	-	-	-	-	-
91	92				-0.20	+0.23				24.3	10.9
92	93	-0.17	+0.11	+0.13	-0.21	+0.14	17.6	4.6	14.9	5.6	7.9
93	94				-0.33	-0.02				12.4	9.7
94	95	-0.22	+0.05	+0.13	-0.12	+0.06	12.2	21.2	19.0	14.3	8.6
95	96				-0.07					5.8	
96	97	-0.10	+0.11	0.00	-0.24	+0.17	25.5	14.5	5.7	15.0	10.9
97	98				-0.31	+0.03				7.1	8.5
98	99	-0.22	+0.09	-0.12	-0.41	+0.12	16.4	12.7	17.5	5.9	11.9
99	100				-0.39	+0.07				6.5	8.2
100	101	-0.50	-0.52	-0.19	-0.74	-0.24	56.0	101.7	10.8	33.1	16.9
101	102				-0.46	-0.29				27.3	12.5
102	103	-0.09	+0.18	+0.15	-0.12	+0.24	82.2	134.0	62.0	32.8	40.2
103	104				-0.40	+0.13				23.9	10.8
104	105	-0.28	-0.06	-0.10	-0.46	+0.02	27.4	51.7	43.3	5.2	7.8
105	106				-0.24	+0.06				18.3	5.4
106	107	-0.02	-0.05	+0.02	-0.21	+0.13	24.5	5.0	23.1	6.2	8.5
107	108				-0.14	+0.21				6.6	7.2
108	109	-0.15	-0.11	-0.02	-0.24	+0.17	12.1	14.1	6.6	7.1	19.2
Mean		-0.17 ± 0.14	-0.01 ± 0.20	0.01 ± 0.12	-0.27 ± 0.18	+0.08 ± 0.14	30.4 ± 23.5	39.9 ± 47.0	22.5 ± 18.6	14.3 ± 9.9	12.1 ± 8.0

R_0 = 6378.166 km

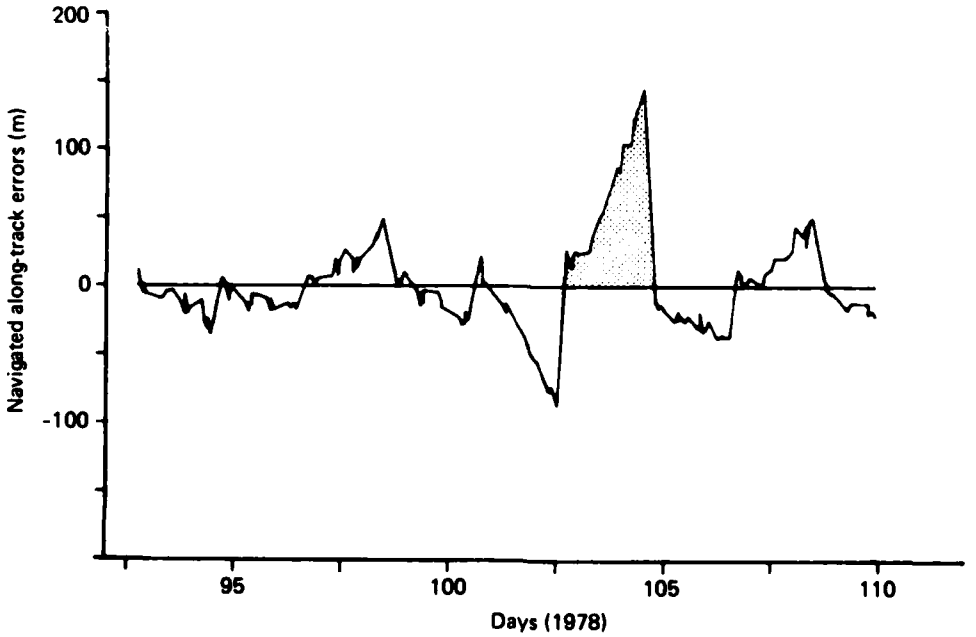

Fig. 4 Along-track navigation residuals for satellite 30120.

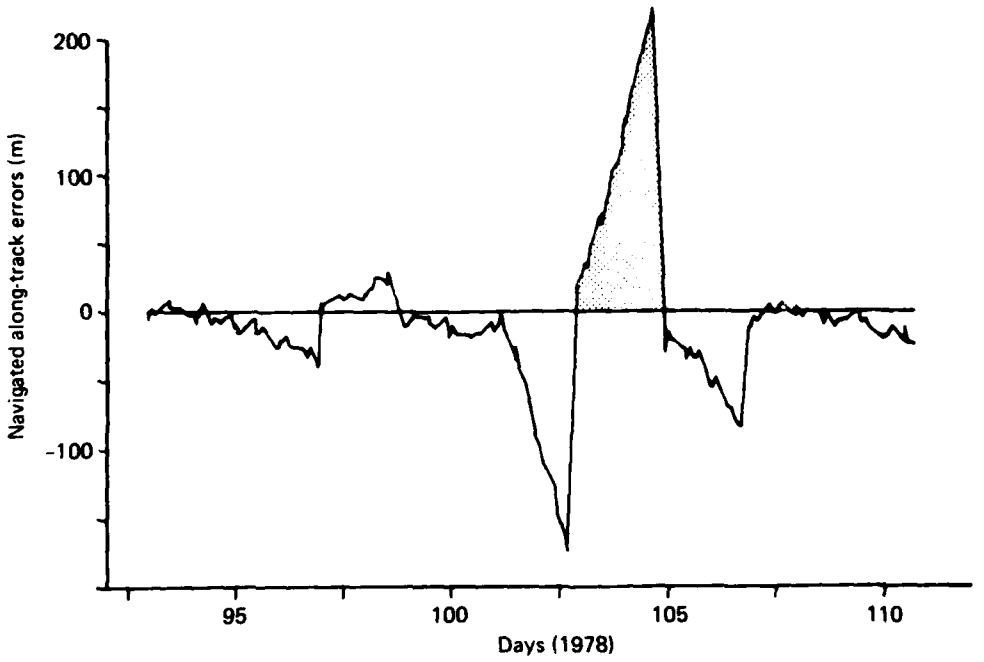

Fig. 5 Along-track navigation residuals for satellite 30130.

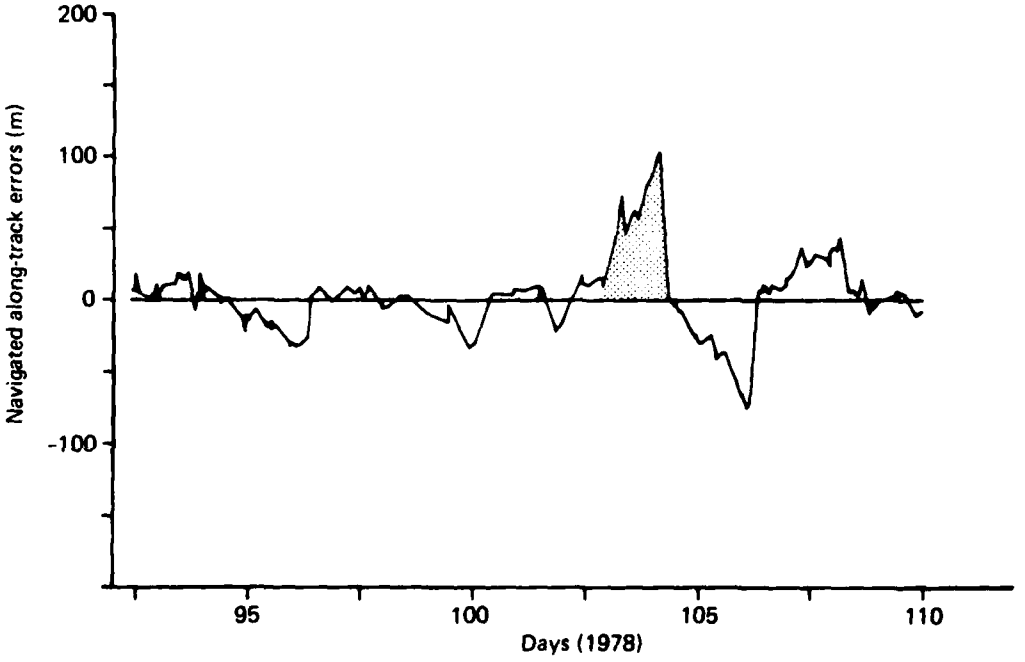

Fig. 6 Along-track navigation residuals for satellite 30140.

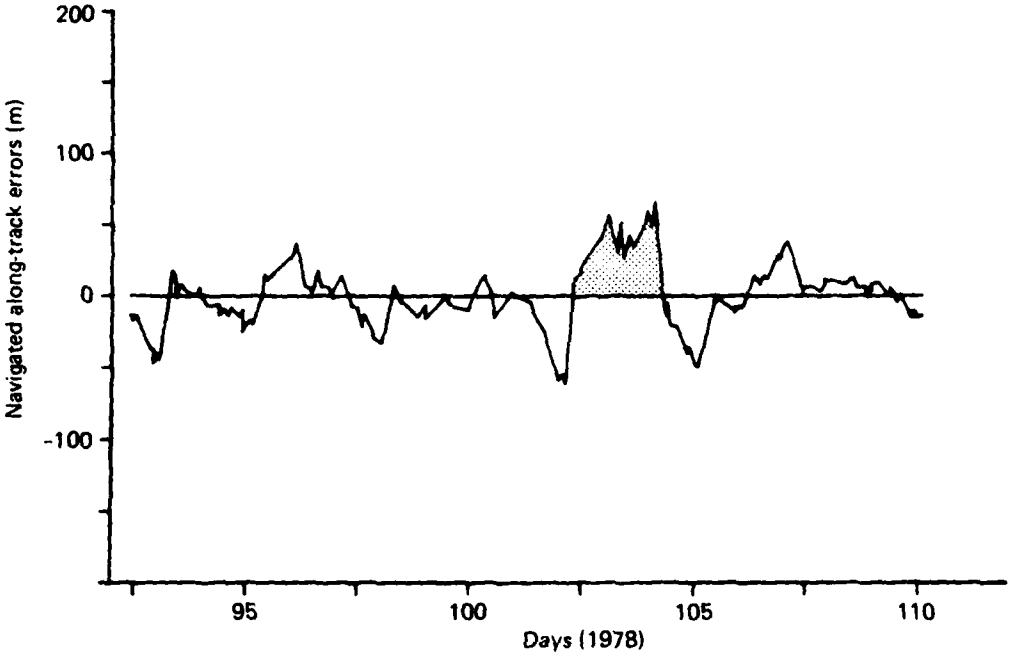

Fig. 7 Along-track navigation residuals for satellite 30190.

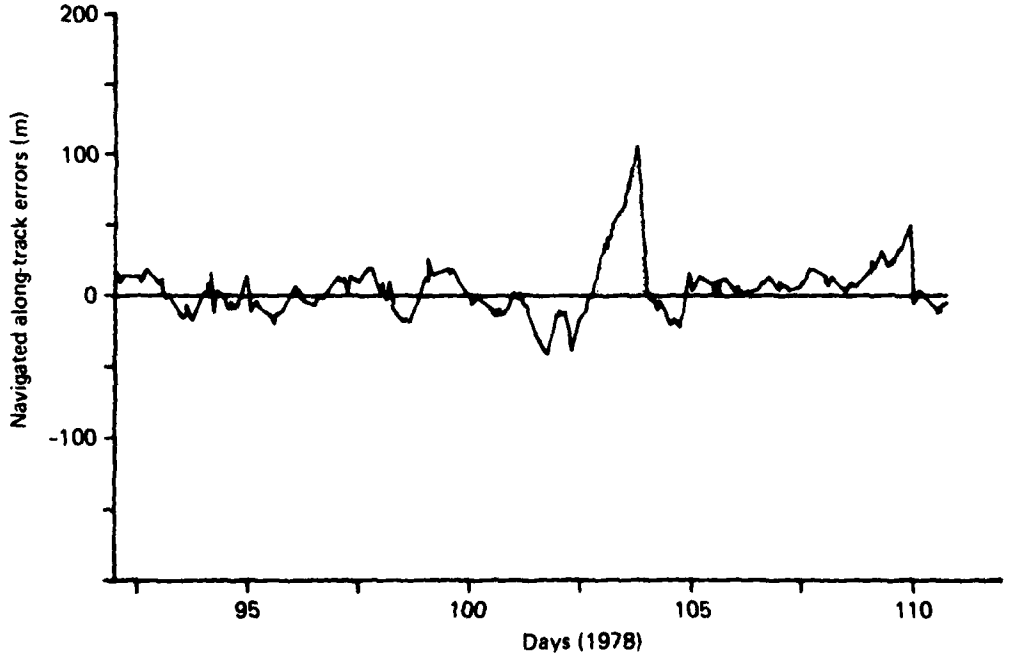

Fig. 8 Along-track navigation residuals for satellite 30200.

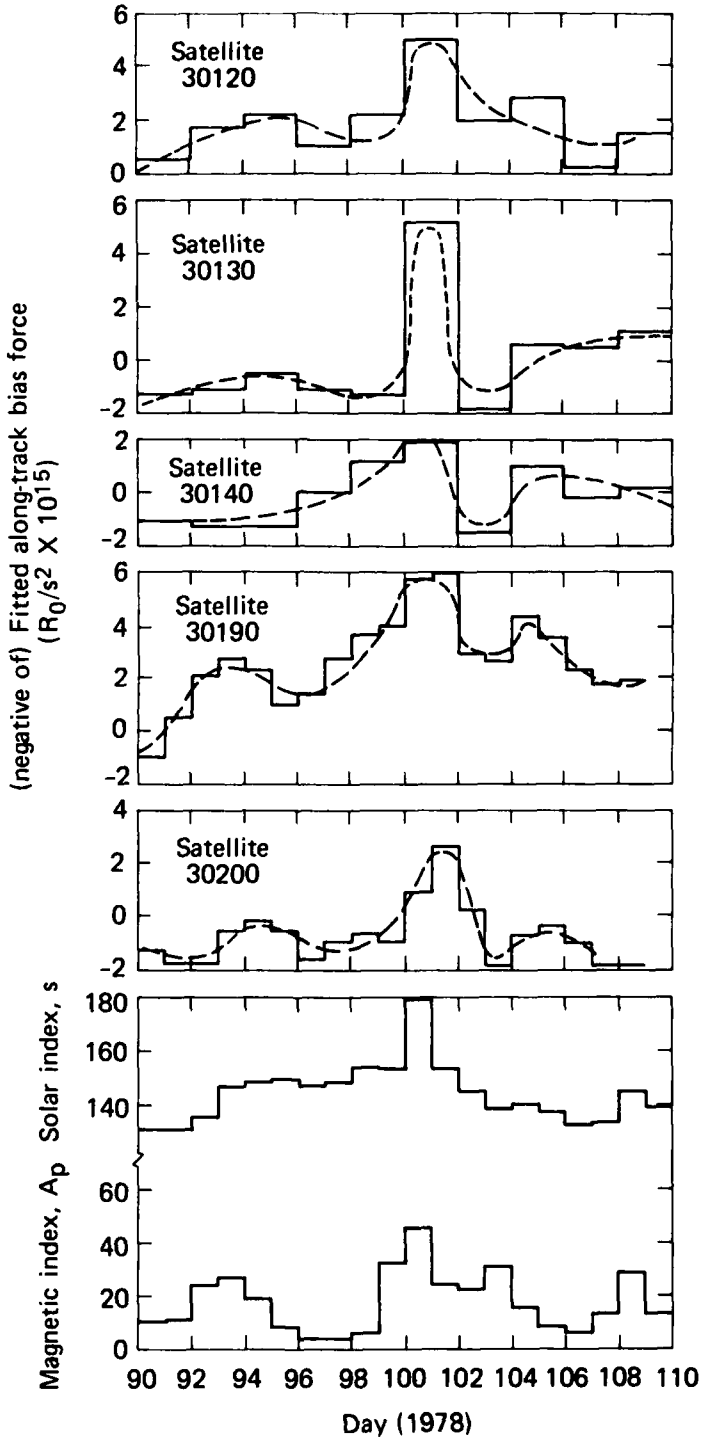

Fig. 9 Fitted along-track bias forces and prevailing solar/magnetic conditions.

can also be observed in the (negative) decline in the fitted bias force on days 105 to 108.

3. The maximum (negative) fitted bias force for all three satellites (days 100 to 101) coincides with the peak daily solar index (s = 180).

We can draw two inferences from the above observations:

1. The drag model underestimates the effects of increased magnetic activity, and

2. The drag model underestimates the effects of daily variations in the solar activity.

The poor performance of the drag model during this period prompted NAVASTROGRU to implement a manual procedure of monitoring the extrapolated along-track position errors daily and periodically adjusting the mean drag force by changing the "true" (nominal) coefficient of drag parameter (C_d = 3.0) either upward (model under-predicting drag) or downward (over-predicting drag).

7. ADDITIONAL RESULTS OF DRAG ESTIMATION

Four additional experiments with drag estimation were carried out over the past year: (a) satellite 30200, days 264 to 304, 1978; (b) satellite 30120, day 340, 1978, to day 15, 1979; (c) satellite 30140, day 344, 1978, to day 15, 1979; and (d) satellite 30190, days 94 to 118, 1979. The last three experiments were carried out by NAVASTROGRU personnel as part of their ODP and drag estimation option checkout.

The results of the first experiment (satellite 30200) are illustrated in Fig. 10. We note the following:

1. The mean of the rms of the along-track errors (48 h interval, the last 24 h extrapolated) was 13.4 ± 8.9 m.

2. The fitted (negative) along-track bias increased steadily over the 40 day span (21 September to 31 October), coinciding with known deficiencies in the modeled semiannual variation in density (the maximum occurring in October) and the absence of the seasonal-latitudinal variation in helium content from the presently implemented drag model (Ref. 2).

3. We note a reasonable correlation between A_p and the fitted bias force ($-F_B$) during a moderate storm (days 268 to 272).

4. Peak fitted bias forces on days 291 to 292 are not preceded nor do they coincide with a magnetic storm (high A_p's), although they do occur two days after maximum reported solar disturbances (s = 180).

5. Manual drag estimation (changing C_d) instituted at NAVASTROGRU following the problems in April 1978 closely paralleled the fitted along-track bias force. C_d varied from 2.8 (less than nominal) at the start of the span to 5.4 (1.8 times nominal) at the end (see item 1 above). The two local peaks in fitted bias force (items 3 and 4 above) have their counterparts in C_d. Although both

---

Ref. 2. A. Eisner and S. M. Yionoulis, "Long-Period Terms in the Neutral Density of the Upper Atmosphere," JHU/APL CP 076, Nov 1979.

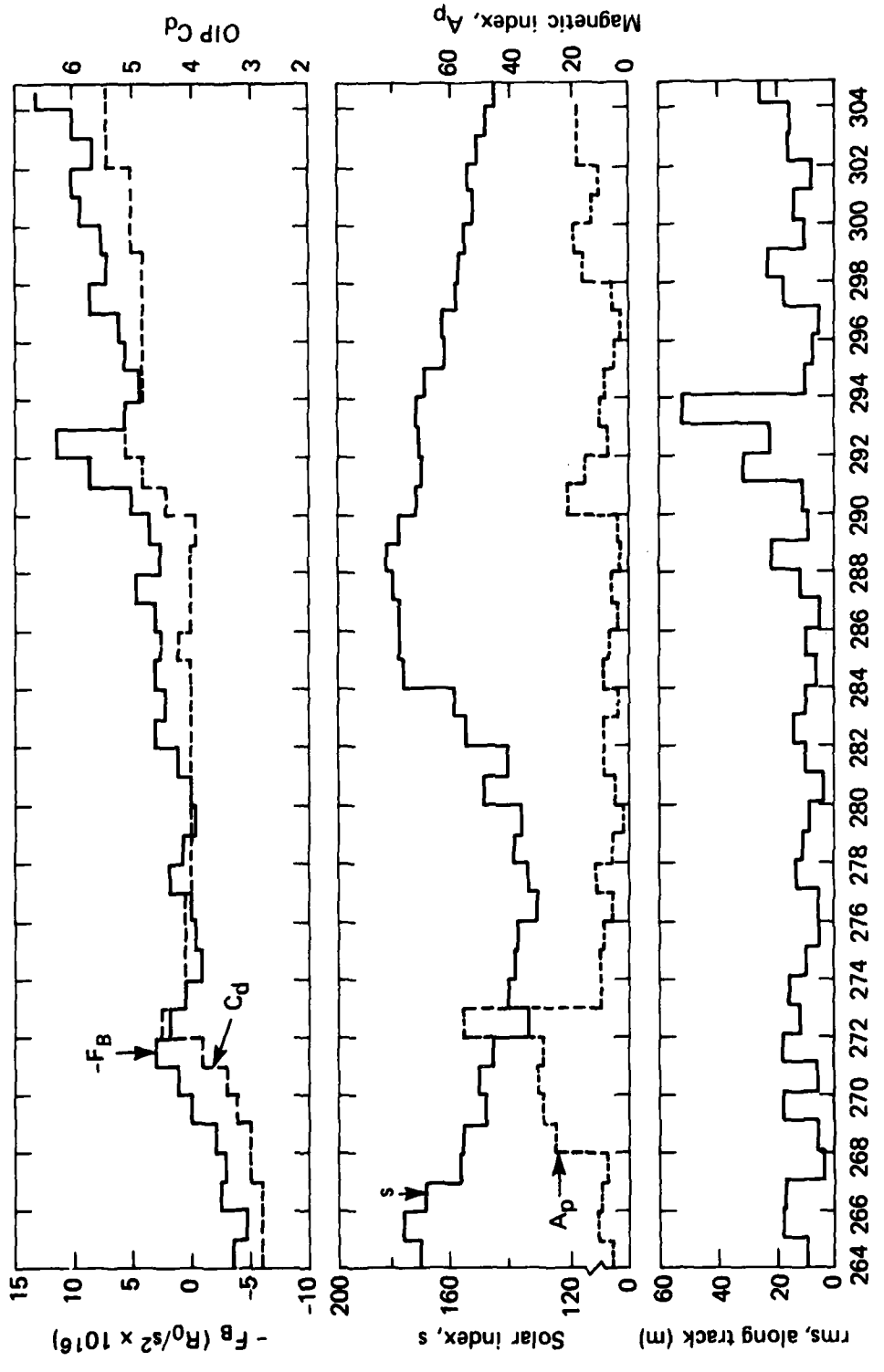

Fig. 10 Fitted along-track bias force (ODP), operationally used C_d (OIP), and prevailing solar/magnetic conditions for satellite 30200.

methods follow the long-period variations well, the fitted bias force is more sensitive to low-level errors and picks up changes earlier than the manual system.

The results of the second experiment (satellite 30120) are illustrated in Fig. 11. We note the following:

1. The mean of the rms of the along-track errors (48 h interval, the last 24 h extrapolated) was 21.3 ± 13.5 m, 8 m worse than the results of the previous experiment. Six of the 41 days had an rms greater than 30 m. Excluding those six, the rms of the remaining 35 days was 16.7 ± 6.7 m. Each of the six poor extrapolations is associated with sudden changes to the fitted along-track bias force. On three of the six days, the changes correlate with the onset or end of a magnetic storm (days 350 to 351, 1978, and day 4, 1979). The balance, particularly days 9 and 12, 1979, correlates with large changes in the fitted along-track bias force ($>4 \times 10^{-16}$ R_0/s^2) of unknown origin.

2. The fitted bias force shows a strong long-period (28 days) oscillation. It is primarily a resonance effect (Ref. 3) resulting from errors in the 27th-order modeled geopotential coefficient. The very pronounced variations in s and associated modeling errors of this effect are probably the other contributions to the periodic variation in F_B.

3. There is a possible correlation between A_p and $-F_B$ during moderate magnetic storms (days 352 to 353).

4. Manual drag estimation (changing C_d) follows the general trend of the fitted bias force but is less detailed (see the first experiment, item 5 above).

The results of the third experiment (satellite 30140) are illustrated in Fig. 12. We note the following:

1. The mean of the rms of the along-track errors (48 h interval, the last 24 h extrapolated) was 13.8 ± 9.1 m, which is more in line with the results of the first experiment. Only two of the 37 days had rms values exceeding 30 m (excluding those two, the mean was 12.4 ± 7.0 m).

Ref. 3. S. M. Yionoulis, "A Study of the Resonance Effects Due to the Earth's Potential Function," J. Geophys. Res., Vol. 70, No. 24, Dec 1965, pp. 5991-5996, and Vol. 71, No. 4, Jan 1966, pp. 1289-1291.

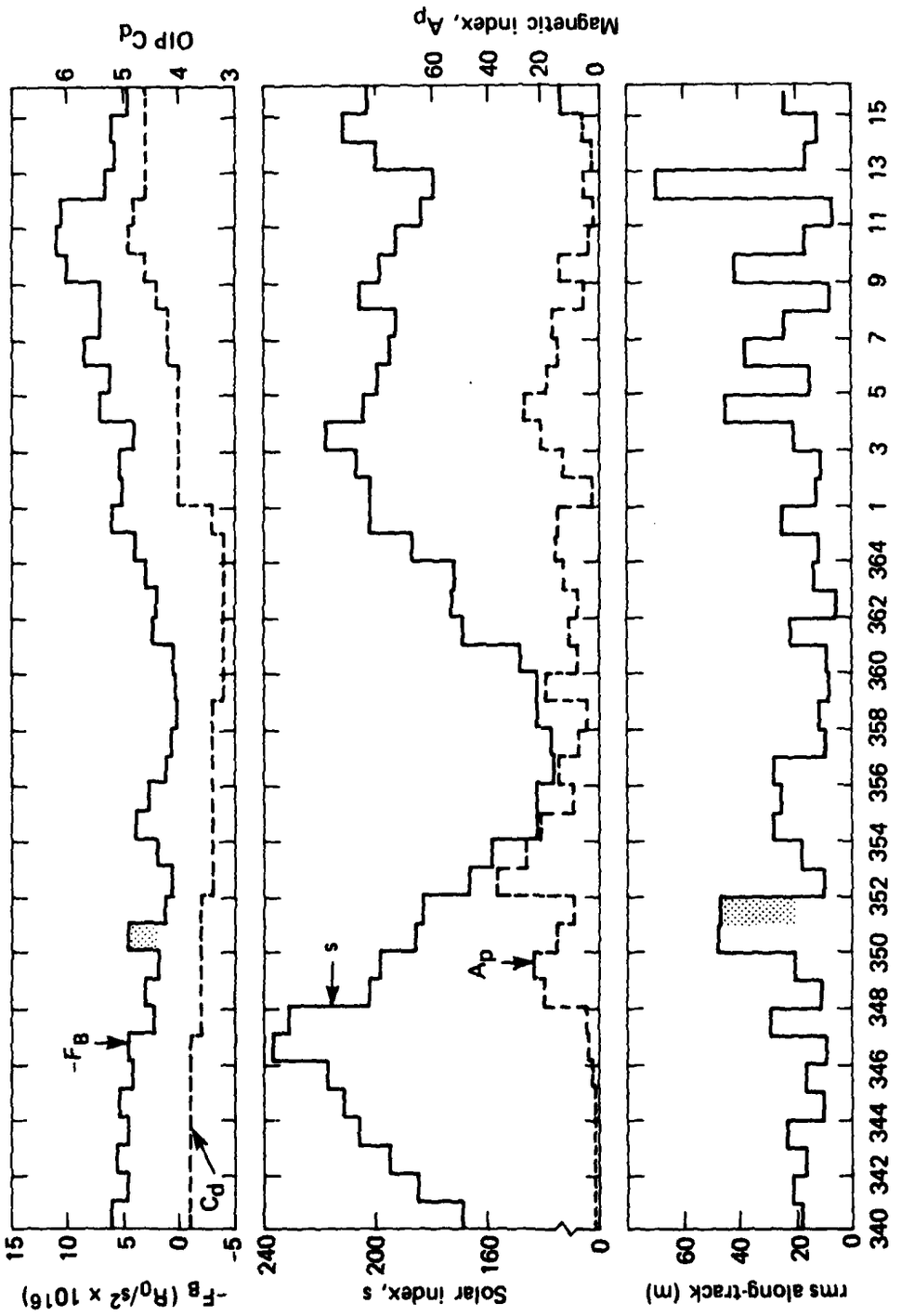

Fig. 11 Fitted along-track bias force (ODP), operationally used C_d (OIP), and prevailing solar/magnetic conditions for satellite 30120.

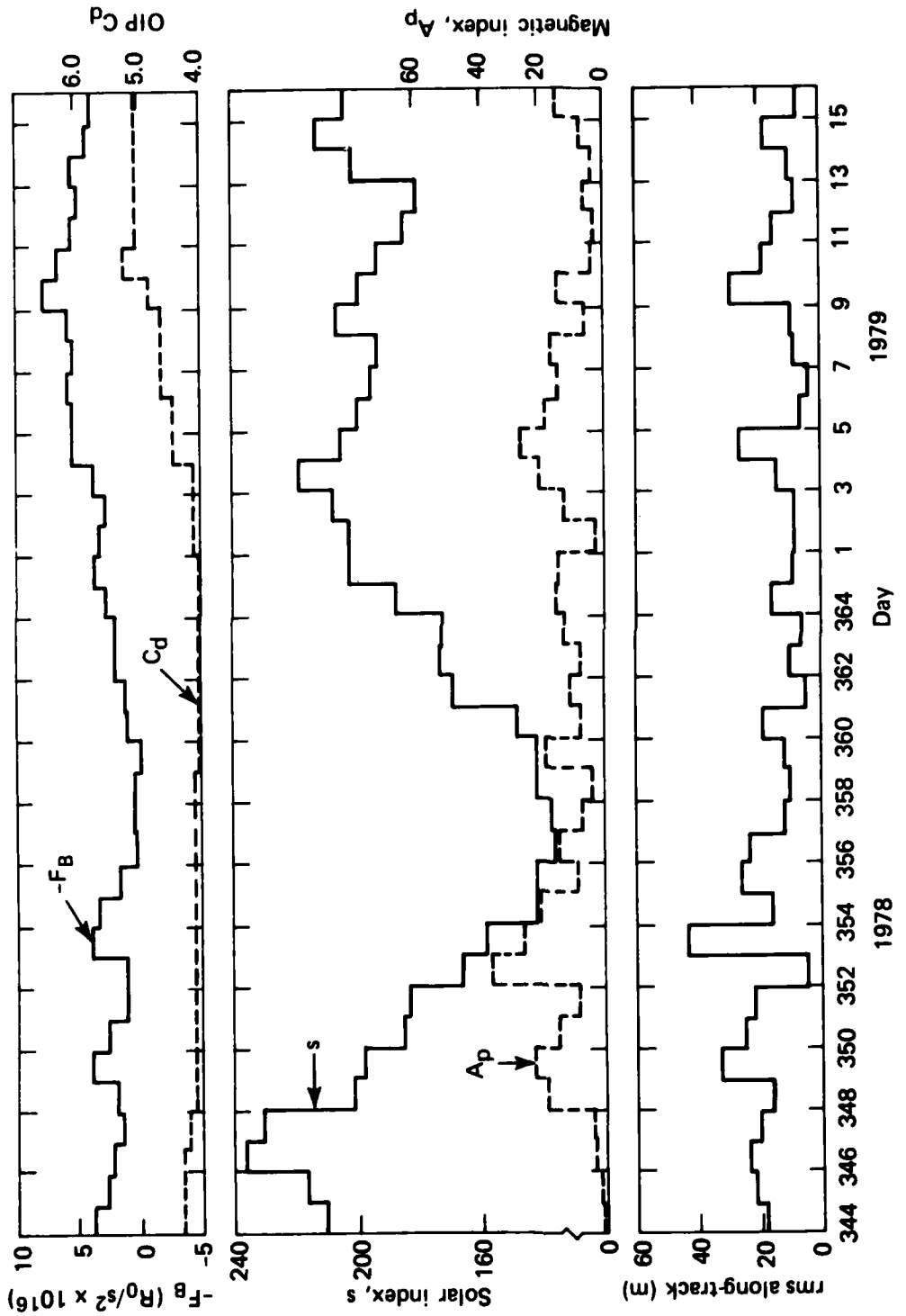

Fig. 12 Fitted along-track bias force (ODP), operationally used C_d (OIP), and prevailing solar/magnetic conditions for satellite 30140.

2. The strong periodic oscillation in the fitted along-track bias force noted with satellite 30120 (the second experiment) is not evident in this satellite. Satellite 30140 is insensitive to errors in the 27th-order modeled geopotential coefficient. The weak periodic oscillation that is present is probably associated with the pronounced variations in s as discussed in the second experiment, item 2.

3. There is a strong suggestion for a correlation between A_p and $-F_B$ (see days 348 to 349 and 352 to 353, 1978, and days 3 to 5, 1979).

4. Manual drag estimation (changing C_d) follows the general trend of the fitted bias force but, once again, it lacks the detailed structure of the latter (see the discussion of the first experiment, item 5).

The set of experiments with drag estimation was completed with the final and most recent data for satellite 30190. One minor revision was made in the drag tracking procedure. In all the previous experiments, no explicit changes to the satellite period were made; that is, there was no linear term in the fitting space. We found that we could achieve better overall results by including the linear term in the fitting space and "binding" changes to the semimajor axis (linear term) to a few centimeters. Results are summarized in Table 6 and illustrated in Fig. 13. We note the following:

1. The mean of the rms of the along-track error was 21.3 ± 23.0 m when fitting an along-track force, compared to 16.5 ± 16.2 m when using manual drag estimation (changing C_d). The reason for the relatively poor performance of the former (when compared to the latter) will be dealt with in the next section.

2. The fitted (negative) along-track bias force decreased steadily over the 25 day span (4 to 28 April), coinciding with the known deficiencies in the modeled semiannual variation in density (the decline from the April maximum) and the absence of seasonal-latitudinal variations in atmospheric helium content from the presently implemented drag model (Ref. 2).

3. A strong correlation is evident between A_p and $-F_B$ on three separate occasions (days 95, 112, and 116). In all three the modeled drag force is too small and is supplemented by sudden increases in the fitted along-track bias force (days 95, 113, and 116).

Table 6

Satellite 30190 in 1979.

Day	Solar index		Magnetic index	No-drag tracking			Drag tracking		
	3 month mean	Daily	A_p	C_d	Along-track rms (m)		$-F_B \times 10^{15}$ (C_d = 3.0)	Along-track rms (m)	
					Prediction	Track		Prediction	Track
94	198	200	21	4.5	18.2	4.7	1.6	19.1	3.2
95	198	183	[40]	4.5	84.0	17.5	2.7	61.7	5.5
96	198	179	13	4.7	10.1	6.0	1.4	[88.1]	3.8
97	197	171	9	4.7	40.0	13.5	0.8	21.1	3.2
98	197	168	8	4.0	16.7	7.3	0.5	19.9	3.2
99	197	170	8	3.8	10.2	3.5	0.6	5.2	3.5
100	197	170	10	3.8	4.8	3.7	0.7	11.2	3.1
101	197	179	5	4.2	9.4	3.9	1.1	17.3	2.9
102	197	170	9	4.2	9.4	3.9	1.0	4.3	3.3
103	197	172	9	4.2	10.9	2.8	0.9	4.1	2.1
104	197	170	11	4.2	13.0	4.5	0.8	7.2	3.3
105	196	167	15	3.8	14.5	5.2	0.4	15.9	2.8
106	196	172	12	3.8	14.0	2.8	0.7	11.5	2.9
107	196	170	12	3.7	9.4	4.4	0.5	20.8	2.5
108	196	157	6	3.7	6.1	3.1	0.5	5.0	2.5
109	195	152	4	3.5	6.8	4.1	0.2	11.7	2.7
110	195	151	1	3.1	26.5	4.4	0.2	8.6	3.0
111	194	165	12	3.1	19.7	5.3	0.3	11.2	2.8
112	193	159	[27]	3.3	5.5	3.2	0.3	5.6	2.9
113	192	162	18	3.6	-	-	0.8	34.1	2.8
114	192	163	14	3.6	8.3	7.1	0.2	[32.2]	3.6
115	191	174	[69]	3.3	11.3	4.3	0.2	8.7	3.6
116	191	178	11	3.7	18.2	10.0	1.2	42.0	3.7
117	191	185	22	3.6	13.7	11.4	-0.3	[74.9]	3.4
118	191	182	31	3.1	16.1	5.9	-0.2	4.4	3.4
				Mean*	16.5 ± 16.2	5.7 ± 3.8		21.3 ± 23.0	3.2 ± 0.6

*Excludes day 113

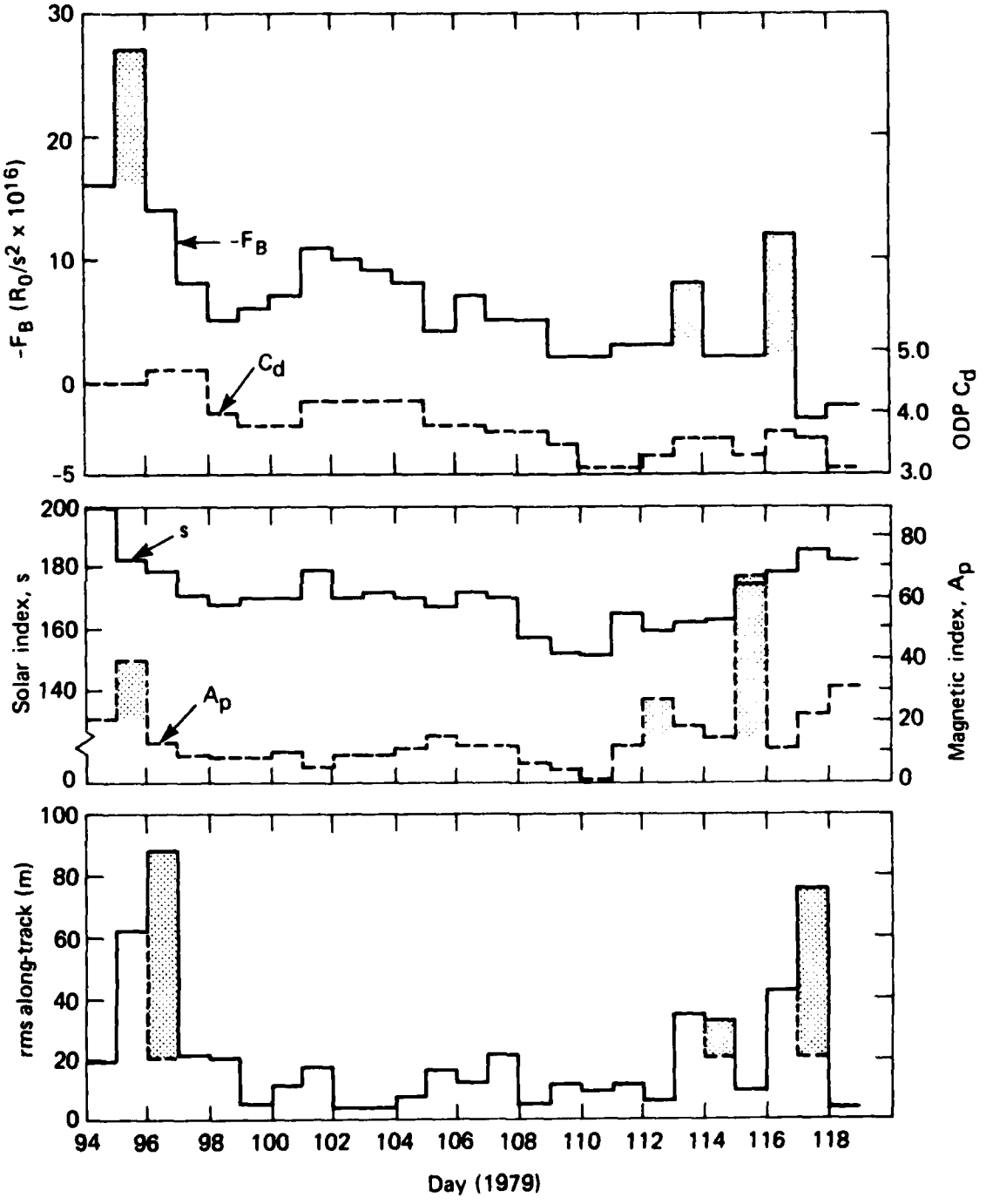

Fig. 13 Fitted along-track bias force (ODP), operationally used C_d (OIP), and prevailing solar/magnetic conditions for satellite 30190.

4. Manual drag estimation (changing C_d) follows the general trend of the fitted bias force but lacks the detailed structure of the latter (see the discussion of the first experiment, item 5).

8. REFINING THE DRAG ESTIMATION TECHNIQUE

The results of the last experiment described in the previous section were surprising. We expected that the computer drag estimation (fitting a bias force) would do better than its manual counterpart of changing C_d. Instead we found that the opposite was true. Let us examine the assumptions that form the basis for computer drag estimation.

The first assumption is that removing the quadratic growth in the along-track position error will result in a more precise set of initial orbit elements that, when integrated, will give a better fit to the data (along-track errors).

The second assumption is that errors in the drag model are slowly varying and that the best guess at tomorrow's force correction is to use today's fitted bias force.

The first assumption is clearly correct. The mean of the rms of the along-track errors in the tracking span of the last experiment (Table 6) was 3.2 ± 0.6 m as compared to 5.7 ± 3.8 m, a 43% reduction in favor of computer drag estimation. The second assumption is only partially correct; that is, although it is generally true that drag model errors are overall slowly varying (see Figs. 9 through 13), it is not always true that the best guess at tomorrow's errors is today's fitted error. The two worst predictions in the last experiment (satellite 30190) on days 96 and 117 (shaded areas in Fig. 13) are a result of using the large (transient) fitted along-track bias force on days 95 and 116 to predict (extrapolate) the satellite's along-track position on days 96 and 117, respectively. There are several other instances, although less dramatic, in the earlier experiments described above. One example was satellite 30120, day 350, 1978, and the extrapolated position errors on the following day (shaded areas in Fig. 11). Another example was the large though transient along-track bias forces (Fig. 9) fitted for days 100 to 101, 1978, associated with solar and magnetic disturbances that, when used in the prediction span (days 102 to 103), resulted in large along-track position errors (shaded areas in Figs. 4 to 8).

In every case we are faced with a large change (greater than 4×10^{-16} R_0/s^2) in the fitted along-track bias force from one track

to the next. The fitted force is correct for the track (orbit determination interval), but it is likely to result in large along-track extrapolated position errors since the source of the change was almost invariably transient in nature (a magnetic storm) and, as a rule, does not persist beyond the tracking span.

A safer strategy for dealing with rapid changes in the fitted along-track bias force is to replace force with a weighted mean of the preceding two to five fitted forces (weighting the most recent most heavily, etc.). Using such a strategy, days 96 and 117 (satellite 30190, 1979, Table 6) were repeated with the fitted forces of 27×10^{-16} R_0/s^2 replaced with 19×10^{-16} R_0/s^2 in the former and 12×10^{-16} R_0/s^2 replaced with 7×10^{-16} R_0/s^2 in the latter. The rms of the prediction improved from 88.1 to 23 m in the former and from 74.9 to 22 m in the latter. The new mean of the rms of the along-track errors was 16.4 ± 13.5 m, a significant improvement of 5 m in the mean and 10 m in the standard deviation. In practice, the strategy described is simple to implement. It is only necessary to keep a daily log of the fitted along-track bias force for each satellite. As a new orbit is determined, the latest fitted force is checked against the log. Whenever the fitted force (new force) differs from the input force (previous run fitted force) by more than 4×10^{-16} R_0/s^2 (in magnitude), it is replaced with a weighted mean of the previous three to four determined forces (from the log), and a new extrapolated ephemeris is generated for subsequent injection into the satellite memory.

ACKNOWLEDGMENT

I owe a special debt to S. M. Yionoulis who developed the necessary theoretical background (HLC equations) for drag tracking and who has been a constant inspiration, providing encouragement, invaluable advice, and assistance in the development and testing of the drag tracking concept.

I would also like to express my gratitude to the management and staff of NAVASTROGRU for the use of their computer and for their generous assistance. Special thanks go to G. Kennedy, D. Locher, M. Crawford, A. Terrameo, and C. R. Payne for their active participation in the drag tracking evaluation experiments.

REFERENCES

1. H. E. Hinteregger, "Development of Solar Cycle 21 Observed in EUV Spectrum and Atmospheric Absorption," J. Geophys. Res., Vol. 84, No. A5, 1 May 1979.

2. A. Eisner and S. M. Yionoulis, "Long-Period Terms in the Neutral Density of the Upper Atmosphere," JHU/APL CP 076, Nov 1979.

3. S. M. Yionoulis, "A Study of the Resonance Effects Due to the Earth's Potential Function," J. Geophys. Res., Vol. 70, No. 24, Dec 1965, pp. 5991-5996, and Vol. 71, No. 4, Jan 1966, pp. 1289-1291.

Appendix A
DRAG ESTIMATION THEORY*

We begin with a set of so-called HLC equations of satellite motion that were derived by W. H. Guier:

$$H'' - (3+10\,\varepsilon\cos M)H - (2+4\,\varepsilon\cos M)L' + (2\,\varepsilon\sin M)L = \frac{F_H}{n^2}$$

$$L'' + (2+4\,\varepsilon\cos M)H' - (2\,\varepsilon\sin M)H - (\varepsilon\cos M)L = \frac{F_L}{n^2}$$

$$C'' + (1+3\,\varepsilon\cos M)C = \frac{F_C}{n^2}\ , \qquad \text{(A-1)}$$

where

H,L,C are the range, along-track, and cross-track position errors, and H'',L'',C'' are the respective associated perturbation accelerations,

F_H,F_L,F_C are the perturbing accelerations in the H,L,C directions,

ε is the satellite eccentricity,

n is the satellite mean motion, and

M is the satellite mean anomaly.

We make the following assumptions:

1. The orbits are circular, i.e., $\varepsilon = 0$; and
2. The force of drag is acting along-track only, i.e., $F_H = F_C = 0$.

*Developed by S. M. Yionoulis

Using these assumptions, Eq. A-1 becomes

$$H'' - 3H - 2L' = 0$$

$$L'' + 2H' = \frac{F_L}{n^2}$$

$$C'' + C = 0 \quad . \tag{A-2}$$

We now integrate the second equation in Eq. A-2,

$$L' + 2H = \frac{F_L}{n^2} \quad , \tag{A-3}$$

and, substituting into the first equation in Eq. A-2, we obtain

$$H'' - 3H - 2\left(\frac{F_L}{n^2} M - 2H\right) = 0$$

$$H' + -2 \frac{F_L}{n^2} M = 0 \quad . \tag{A-4}$$

The solution of Eq. A-4 is

$$H = 2 \frac{F_L}{n^2} M \quad . \tag{A-5}$$

Substitute Eq. A-5 into Eq. A-3,

$$L' + 4 \frac{F_L}{n^2} M = \frac{F_L}{n^2} M \quad ,$$

and by integrating we obtain

$$L = -3/2 \frac{F_L}{n^2} M^2$$

$$H = 2 \frac{F_L}{n^2} M \quad . \tag{A-6}$$

The next step is to arrive at an expression relating F_L to one of the drag parameters (C_d). F_L is the error in the modeled drag force. We do not propose abandoning the drag model but rather supplementing it with drag estimation.

We can write the following relation for the error in the modeled drag acceleration, F_L:

$$F_L = 1/2\ A/M\ \langle\rho\rangle\ V^2(C_d - C_{d_0}) \quad , \tag{A-7}$$

where

A/M is the area-to-mass ratio for the satellite,

$\langle\rho\rangle$ is the average density over the tracking span,

V is the average satellite velocity over the tracking span,

C_{d_0} is the input coefficient of drag, and

C_d is the adjusted (tracked) coefficient of drag.

The actual parameter used in the fitting process (a_6) is related to F_L as follows:

$$a_6 = -3/2\ \frac{F_L}{n^2} \quad , \tag{A-8}$$

and the correction to C_d using Eqs. A-7 and A-8 is

$$\Delta C_d = C_d - C_{d_0} = -4/3\ \frac{n^2\ a_6}{A/M\ \langle\rho\rangle\ V^2} \ .$$

The concept of drag estimation was later generalized to fitting out an along-track bias force F_B and integrating the force explicitly rather than implicitly via the change in C_d. Note that changing C_d is not the same as using F_B. The latter (F_B) is a constant force, whereas the former is a varying (following the variations in ρ) force whose mean approximates F_B.

INITIAL DISTRIBUTION EXTERNAL TO THE APPLIED PHYSICS LABORATORY*

The work reported in TG 1327 was done under Navy Contract N00024-78-C-5384. This work is related to Task S1XO, which is supported by Strategic Systems Project Office (SP-243).

ORGANIZATION	LOCATION	ATTENTION	No. of Copies
DEPARTMENT OF DEFENSE			
DTIC	Alexandria, Va. 22314		12
Defense Mapping Agency	Washington, D.C. 20315	Code 52321	1
	St. Louis ATS, Mo. 63118	L. Decker	1
Department of the Navy			
NAVPRO	Laurel, Md. 20810		1
NAVSEASYSCOM	Washington, D.C. 20362	SEA-003	2
Strategic Systems Project Office	Washington, D.C. 20376	SP-24	1
		SP-243	1
NAVASTROGRU	Pt. Mugu, Calif. 93042	Comm. Off.	1
		C. R. Payne	1
		M. Crawford	1
		A. Terrameo	1
		G. Kennedy	1
		D. Locher	1
		T. Smith	1
NSWC	Dahlgren, Va. 22448	R. J. Anderle	1
Department of the Air Force			
AF Geophysics Lab.	Hanscom Field, Bedford, Mass.	H. E. Hinteregger	1
DEPARTMENT OF COMMERCE			
NOAA	Rockville, Md. 20852	B. Chovitz	1
		W. Strange	1
		S. W. Henricksen	1
U.S. GOVERNMENT AGENCIES			
National Aeronautics and Space Administration			
Goddard Space Flight Center	Greenbelt, Md. 20771	J. Marsh	1
		Code 932.0	1
		Code 900.0	1
		Code 621.0	2
CONTRACTORS			
EG&G, Wolf R&D	Riverdale, Md. 20840	W. T. Wells	1
		S. Klosko	1
UNIVERSITIES			
Stanford University	Stanford, Calif. 94305	D. B. Debra	1
Ohio State University	Columbus, Ohio 43210	R. H. Rapp	1
Augsburg College	Minneapolis, Minn. 55455	M. J. Engebretson	1
MISCELLANEOUS			
Geodetic Survey of Canada, Dept. of Energy, Mines, and Resources	Ottawa, Canada	J. Kouba	1
Bedford Institute	Halifax, Nova Scotia	D. Wells	1
Institut fur Angewandte Geodasie	Federal Republic of Germany	P. Wilson	1
Smithsonian Astrophysical Observatory	Cambridge, Mass.	L. Jacchia	1
		J. Slowey	1
Royal Aircraft Establishment	Farnborough, Hants., England	D. G. King-Hele	1
		G. E. Cook	1
		D. Scott	1
Bureau Central de l'Association Internationale de Geodesie	Paris, France	I. L. Mueller	1

Requests for copies of this report from DoD activities and contractors should be directed to DDC, Cameron Station, Alexandria, Virginia 22314 using DDC Form 1 and, if necessary, DDC Form 55.

*Initial distribution of this document within the Applied Physics Laboratory has been made in accordance with a list on file in the APL Technical Publications Group.

Preceding Page Blank